Sonochemical Modification of Carbon Nanotubes for Enhanced Nanocomposite Performance

Gareth J. Price*[a], Mohsan Nawaz[b], Tariq Yasin[c], Saira Bibi[b,c]

a. *Department of Chemistry, University of Bath, Claverton Down, Bath, BA2 7AY, UK*
b. *Department of Chemistry, Hazara University, Mansehra, Pakistan.*
c. *Pakistan Institute of Engineering and Applied Sciences, Islamabad, Pakistan*

* Corresponding author.

Correspondence regarding the paper (GJP): g.j.price@bath.ac.uk, +44 (0)1225 386504

Abstract

Multi-walled carbon nanotubes (CNTs) have been treated using 20 kHz ultrasound in combination with dilute nitric and sulfuric acids at much lower concentrations than previously reported. The measurements revealed an optimum set of sonication conditions (in this case 30 min at 12 W cm^{-2}) exists to overcome aggregation of the nanotubes and to allow efficient dispersion in ethanol or in chitosan. Transmission electron microscopy and Raman spectroscopy suggested the removal of amorphous material and reduction of the CNT diameter as well as modifications to their defect structures. The surface oxidation was determined by FTIR spectroscopy. At longer times or higher ultrasound intensities, degradation such as nanotube shortening and additional defect generation in the graphitic network occurred and the benefits of using ultrasound decreased. The modified CNTs were used as fillers for chitosan films and gave a tenfold increase in tensile strength and integrity of the films. The methodology was combined with sonochemical generation of gold or iron oxide nanoparticles to produce a range of functional membranes for catalytic reductive hydrogenation or dye degradation under conditions that are more environmentally benign than those previously used. Our results further add to the usefulness of sonochemistry as a valuable tool in preparative materials chemistry but also illustrate the crucial importance of careful control over the experimental conditions if optimum results are to be obtained.

Graphical abstract

Sonochemical modification of carbon nanotubes has been performed under mild conditions and combined with sonochemical nanoparticle synthesis to prepare a range of functional chitosan membranes.
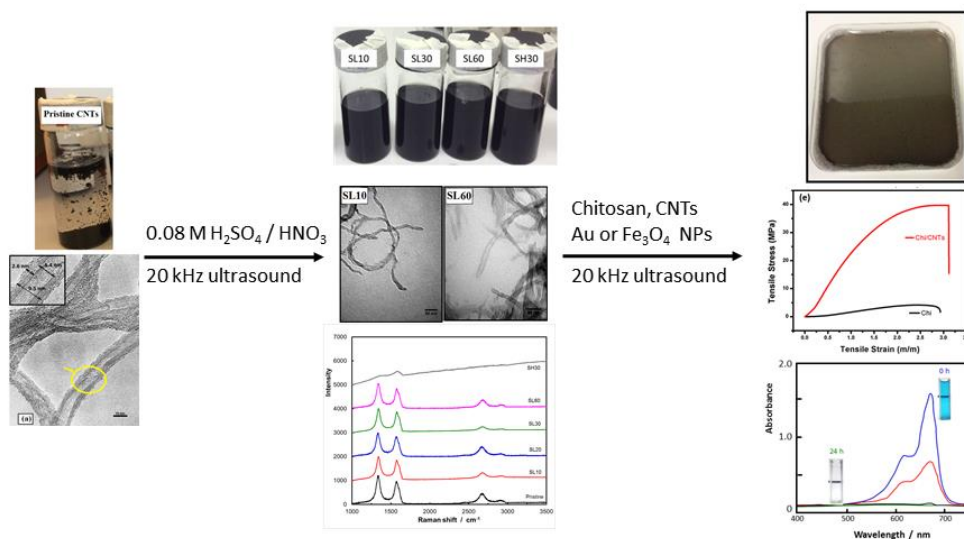
Highlights

- A systematic study of sonochemical modification of multi-walled carbon nanotubes (CNTs) is presented
- 20 kHz ultrasound allows dilute acid modification at lower concentrations than reported previously
- TEM and Raman spectroscopy reveal changes to the CNT microstructure; FTIR reveals their surface chemistry
- An optimum set of conditions occur for promoting CNT modification
- Modifying the CNTs greatly enhances the mechanical properties when incorporated into chitosan films
- Sonochemically generated nanoparticle (*e.g.* Au, Fe_3O_4) can also be incorporated to give catalytically active membranes

1. Introduction

Carbon nanotubes, CNTs, have a unique set of properties and have found use in a vast range of applications [1-3]. On account of their extraordinary mechanical strength, nanometer size, high aspect ratios and exceptionally high electrical and thermal conductivity, CNTs have also been used as reinforcing fillers to enhance the mechanical properties and functionality of synthetic and natural polymers [4-6]. However, CNTs are very hydrophobic and are difficult to disperse in polymer matrices since they readily aggregate due to strong van der Waals interactions [7, 8] so they have to be functionalised prior to use. Functionalisation can be performed by coating with surfactants, high-energy (*e.g.* γ-ray) irradiation or by chemical etching with strong oxidising agents or concentrated acids [9]. In previous work, CNTs were irradiated in air to a dose of 100 kGy under γ-irradiation from a Co-60 source which allowed effective dispersion of CNTs into chitosan films [10]. However, this procedure involved long reaction times to achieve efficient results (*e.g.* four days) as well as requiring access to a gamma source. Surface functionalization of CNTs was also attempted using acidic reflux but this also required prolonged treatment, often as long as three days.

To reduce the severity of the reaction conditions necessary for CNT modification, sonochemical modification has recently been studied [11, 12]. Among its many other applications, sonochemistry has also been widely applied in the synthesis of polymers and nanoparticles [13, 14]. Using high power ultrasound offers a potentially facile and versatile tool for surface functionalization/oxidation of nanotubes, lowering the reaction time and overall energy requirements. The major effects arise from acoustic cavitation, where the formation, growth and implosion of bubbles in the liquid generates reactive intermediates such as hydroxyl radicals as a result of solvent breakdown due to high pressures (~1000 bar) and temperatures (~

5000 K). Shock waves and microjets also occur which could overcome the interactions causing aggregation to disperse the CNTs and also generate deformities on the nanotubes leading to functional groups being formed on their surfaces. These features have been shown to play a crucial role in surface functionalization [15]. However, questions still remain as to the most effective treatment regimes and optimum conditions under which to perform the reactions, hence the work reported here.

Our work in modifying and dispersing CNTs is aimed at producing functional polymer films and membranes [16, 17]. In this work, chitosan has been used as the polymer matrix. Chitosan (Chi) is a non-toxic polysaccharide that displays excellent biocompatibility, biodegradability and can readily form films by casting from solutions in acidic media [18]. Chi/CNT nanocomposites have received increasing attention in view of their attractive structural, mechanical and electrical properties [16, 19, 20], with potential uses in tissue engineering, biomedicine, catalysis, sensor and biosensor applications.

However, unfilled chitosan films are brittle and lack mechanical strength. The poor tensile properties can be improved by blending or by adding a suitable filler, for which CNTs have been shown suitable [18, 19]. The properties of Chi/CNT nanocomposites depend critically on how well the CNTs can be dispersed into the chitosan matrix [10]. The presence of amine groups in chitosan promotes the formation of hydrogen bonding between the functionalized CNTs and Chi leading to improvement of the CNTs dispersability and hence to the properties of the films formed from the nanocomposites. Substantial efforts are now being made to adjust the CNT surface to enhance their processability and the performance of the nanocomposites.

In the current study a rapid, direct sonochemical method involving very dilute acids (H_2SO_4/HNO_3) combined with 20 kHz ultrasound has been used to functionalize CNTs. The

effect of different reaction conditions (*e.g.* time and ultrasound intensity) on the CNT structure has been measured. Chi/CNT nanocomposite films have been prepared and CNTs characterised using high resolution TEM together with FTIR and Raman spectroscopies in order to establish the principles on which the sonochemical effects are based. The application of these effects is then illustrated by the potential of these films to incorporate functional nanoparticles such as gold or iron oxide, for catalytic applications in reductive hydrogenation or dye degradation is also described.

2.   Experimental Section

2.1 Chemicals and materials

Multi-walled carbon nanotubes, CNTs, produced by catalytic carbon vapour deposition (9.5 nm average diameter, 1.5 µm average length, purity 90 % by TGA, NC700 series) were purchased from NANOCYL[TM] and used as received. Chitosan (C3646, 75 % deactylated), poly(vinyl alcohol) (PVA, Mw: 146,000-186,000) and poly(vinyl pyrrolidone) (PVP, Mw: 40, 000), were from Sigma-Aldrich (UK) and used without further purification as were all other chemicals and reagents used.

2.2 Sonochemical modifications of CNTs

Raw CNTs (20 mg) were suspended by gentle shaking in 36 cm^3 of a mixture of H_2SO_4 and HNO_3 with the concentration of both acids at 0.08 mol dm^{-3} and sonicated with an ultrasonic horn (Sonic processor L500-20, 20 kHz, 1 cm dia. horn). The temperature was maintained at 60 °C and sonication conducted for varying periods of time at 12 W cm^{-2} (measured calorimetrically [21]) or with varying intensity for a fixed time of 30 min.

2.3 Synthesis of Chi/CNTs nanocomposites

Chitosan (1.8 g) was dissolved in 100 cm^3 of 2% (w/v) acetic acid. PVA with 1.25 mg of CNTs and PVP (10 mg each) were separately dissolved in 10 cm^3 water. The solutions were mixed and vinyl triethoxy silane (15.5 µL) and potassium persulfate (12.5 mg) added before addition to the chitosan solution. After sonication using the same horn as above at 12 W cm^{-2} for 1 h at 45°C, the solution was poured into dishes and allowed to dry to form films at room temperature.

Gold nanoparticles, Au-NPs, were synthesized by sodium citrate (0.05 M) reduction of gold chloride, HAuCl$_4$, (1.25 × 10^{-4} M, 300 cm^3) to insoluble Au(0) [17]. Iron oxide nanoparticles, Fe$_3$O$_4$-NPs, were synthesized by vigorous stirring under nitrogen of FeCl$_3$.6H$_2$O (5.4 g) and FeCl$_2$·4H$_2$O (2.0 g) in acidic solution with deoxygenated NH$_4$OH (250 cm^3, 1.5 M). The black precipitate was isolated from the solvent via magnetic decantation. Washing with water and decantation was repeated three times followed by washing twice with trimethyl ammonium hydroxide (100 cm^3, 0.1 M). Finally, the suspension was washed with acetone and methanol and dried in a desiccator overnight.

Nanocomposite films containing Au-NPs or Fe$_3$O$_4$-NPs were prepared using the above procedure but including the NPs with the PVP solution using the ultrasound horn (10 min at an intensity of 12 W cm^{-2}) before mixing with the PVA solution.

2.4 Measurements and characterization

Samples were suspended by shaking in ethanol and coated onto a holey carbon grid supported on 300 mesh copper. TEM measurements were carried out on a JEOL JEM 1200 EXII instrument operated at an accelerating voltage of 120.0 kV with samples coated on a 200 mesh carbon-coated Cu-grid. High-resolution transmission electron microscopy (HR-TEM) was carried out with a JEOL 2010 instrument, having a point resolution of 0.19 nm and operated at an accelerating voltage of 200 kV. Images were recorded photographically.

Raman spectra from 300 cm^{-1} to 4000 cm^{-1} were recorded at room temperature under ambient conditions using a Renishaw inVia Raman microscope with 532 nm (Diode pump solid, DPSS) green laser with a charge coupled device detector. FTIR spectra were recorded using a Perkin Elmer spectrometer (spectrum 100) at room temperature at scanning range of 4000-500 cm^{-1} (number of scans: 16, resolution: 8.0 cm^{-1}). UV-visible spectra were recorded on an Agilent-8453 spectrophotometer using a quartz cell with path length 0.10 cm.

Tensile tests on the films were carried out at room temperature using an Instron model 3369 material tester. A 100 N load cell was used with an extension rate of 2 mm min^{-1}. The samples were cut into dumbbell shape with dimensions 30.3 mm $\times$ 0.12 mm $\times$ 5.5 mm.

3   Results and discussion

3.1 Effect of ultrasound on CNT structure

Fig. 1 shows TEM images of sonochemically treated CNTs as well as an untreated sample. Before treatment, the CNTs are entangled and interact with each other. Sonication at 12 W cm^{-2} in the dilute acids leads to less entanglement up to around 30 min treatment (SL30) where the sample was well dispersed and individual tubes were well separated. Shorter treatment times did

not fully disperse the nanotubes while after extended times the nanotubes began to re-aggregate. This was also true when the intensity was increased to 18 W cm^{-2} with the additional effect that the average length of the CNTs were shortened. Huang *et al.* also reported that sonication assisted functionalization of CNTs with a polymer also resulted in shortening of the nanotubes depending on the duration of sonication [22]. At the higher intensity, considerable damage was caused to the CNTs and they formed agglomerates of shorter tubes. So, although care must be taken to select the optimum conditions, dispersion of CNTs can be carried out with sonochemical assistance at much lower acid concentrations than are usually used and can hence offer a csafer, more environmentally friendly method.
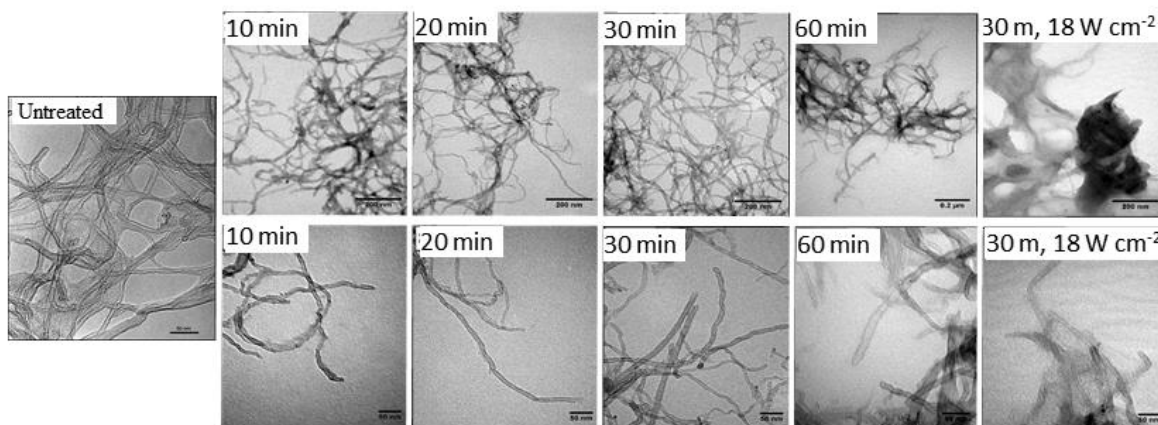

Figure 1: TEM micrographs of untreated CNTs and sonochemically treated CNTs (12 W cm^{-2} except where indicated). Scale bars: 0.2 μm (upper images), 50 nm (untreated and lower images)

Further detail on the structural changes to the CNTs was gained by recording high resolution TEM images of representative samples from the same batch before and after sonochemical treatment. The bundled structure of hollow CNTs is clear for the untreated CNTs in Fig. 2. The nanotube diameters were around 10 ± 0.5 nm with an inner tube diameter

averaging ~ 5.4 nm. The tubes comprised up to seven layers. In some areas of their surfaces, a coating of amorphous carbon can also be observed which had not removed during washing and sample preparation (see below). After 30 min sonochemical treatment at 12 W cm^{-2} (Fig. 2(b)), the average diameter had increased somewhat with the wall thickness of this sample, ~4 nm, also increasing. Of course care must be taken in drawing too definite quantitative conclusions as these measurements were obtained from representative samples from the same batch rather than identical individual nanotubes. The agglomeration and fragmentation occurring after longer treatment times up to 60 min (Fig. 2(c)) is clearly shown along with thinner walls and larger core.

Cavitation also produces a large degree of turbulence and motion and the high shear forces generated break the CNTs, shortening the average length and leading to more open ends [11]. This is even more obvious when a higher ultrasound intensity was used (18 W cm^{-2}, Fig. 2(d)) together with an increase in surface roughness which can be attributed to the etching of CNTs surface by the acids. This process is slow under reflux but Yang *et al.* reported [23] that oxidation is faster under sonication although severe surface etching can result. In our work, much shorter sonication times were involved and did not cause such severe damage except when operating the ultrasonic horn at high intensity.

Information on the extent of oxidation can be gleaned from the infra-red spectra of the CNTs shown in Fig. 3. Spectra of untreated CNTs display no significant levels of functionality. However, sonochemical treatment results in several peaks appearing in the spectra corresponding to a variety of oxygen functionalities. After only 10 min treatment at 12 W cm^{-2} , peaks can be observed at ~2970 cm^{-1}, attributable to C—H stretches, and ~1430 cm^{-1} and ~1070 cm^{-1} arising from C—O bonds. Longer treatments or higher intensities introduce a broad O—H absorption

above 3000 cm^{-1} as well as indications of carbonyl, C=O, and unsaturated C=C absorptions around 1600-1650 cm^{-1}. Each of these peaks is consistent with the acid etching of the CNT surface to introduce polar functionality which should assist in the dispersion within a solvent or a polymer matrix.

Analysis of Raman spectra has proved invaluable in the determination of structural changes in CNTs [24]. The Raman spectra from the pristine and modified CNTs in this work are shown in Fig. 4. Each spectrum displays three prominent peaks at around 1335 - 1366 cm^{-1},
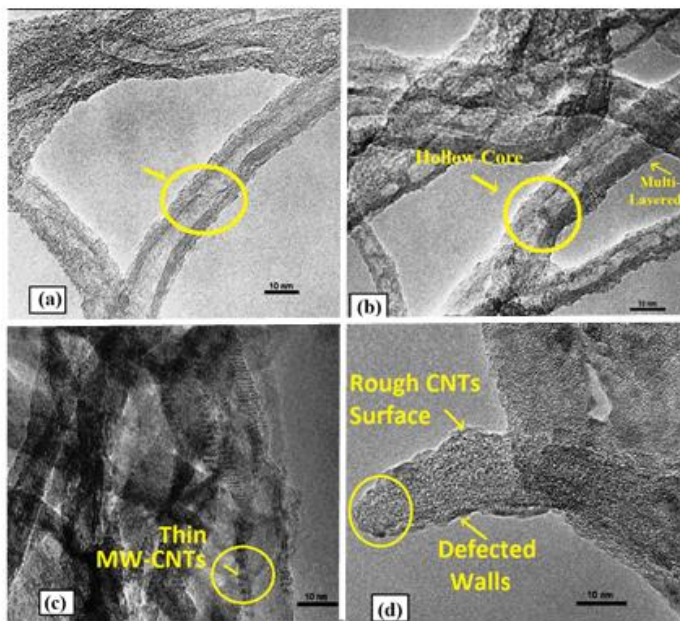

Figure 2: High resolution TEM images for CNTs: (a) untreated; (b) 30 min at 12 W cm^{-2}; (c) 60 min 12 W cm^{-2}; (d) 30 min at 18 W cm^{-2}.
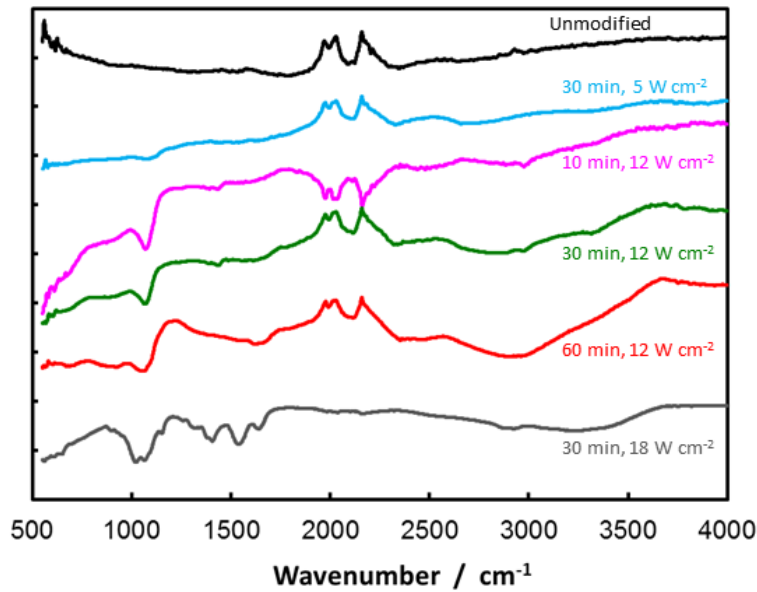
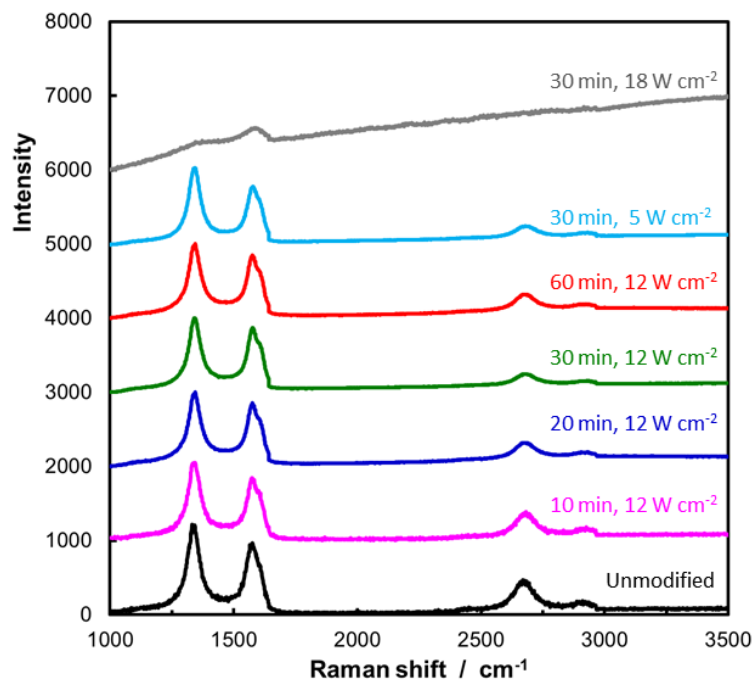**Figure 3:** FTIR spectra of sonochemically treated CNTs.

Figure 4: Raman spectra of CNTs. All the spectra have been normalized with respect to the intensity of the G-band. The intensity (arbitrary units) has been shifted up by 1000 for successive spectra.

1570 - 1581 cm^{-1} and 2667-2682 cm^{-1} corresponding to the D, G and 2D bands respectively. The D-band is characteristic of disordered, defect structures while the G-band is generally assigned to well-ordered sp^2 carbons in a graphite-like structure [25]. Hence, the ratio of the peak intensities, I_D/I_G, is an indication of the degree of disorder and the number of defects in the material and hence the ratio will change with chemical processing. The values recorded in this work are shown in Table 1 along with positions of D and G bands and the I_D/I_G ratios.

For the unmodified CNTs, the I_D/I_G ratio was 1.556, indicating a large amount of amorphous carbon and/or existence of defects in the starting materials even before treatment. After ultrasonic treatment in dilute acid, the I_D/I_G ratio decreased. One potential explanation might be due to the removal of some of the amorphous carbon which can be seen coating the unmodified CNTs but which could possibly be removed as a result of cavitation although again it should be noted that comparison of the same individual CNT is not possible.

Table 1: Raman D and G-band positions and I_D/I_G ratios for pristine and treated CNTs.

Sample conditions	Wavenumber / cm^{-1}			I_D/I_G ratio
	D-band	G-band	2D-band	
Untreated	1338	1577	2674	1.56
10 min, 12 W cm^{-2}	1343	1579	2677	1.55
20 min, 12 W cm^{-2}	1342	1581	2680	1.50
30 min, 12 W cm^{-2}	1343	1581	2684	1.48
60 min, 12 W cm^{-2}	1341	1580	2680	1.60
30 min, 18 W cm^{-2}	1342	1580	2680	1.48
30 min at 5 W cm^{-2}	1341	1580	2683	1.49

After sonochemical oxidation the G-band is also shifted towards higher wavenumber, indicating a reduction of graphitized structures in the CNTs. Chemical reactions such as oxidation may also take place at defect sites. It was noticeable that the I_D/I_G ratio increased after extended treatment time due to the introduction of extensive defects and structural disorder, in part due to the large degree of breakage noted above and the increase in open ends as well as extensive surface reaction. These can result from direct action of the shock waves and shear effects as well as reaction with sonochemically generated radicals and enhanced acid etching.
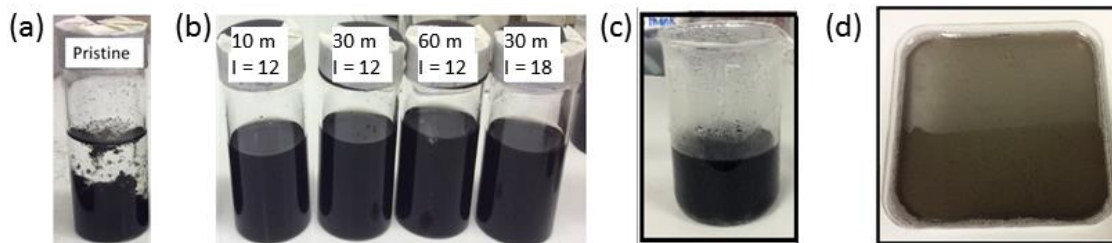

Figure 5: Dispersion of CNTs in ethanol ((a) before and (b) after treatment for varying times, I = intensity in W cm^{-2}) and in chitosan (30 m at 12 W cm^{-2} in (c) solution and (d) in the drying membrane).

The purpose of the surface modification is to allow the effective dispersion of the CNTs in a nanocomposite matrix. Fig. 5 illustrates samples of CNTs distributed in ethanol by vigorous shaking and left to settle for 24 hr. The unmodified CNTs are largely agglomerated and settled after 24 hr. Indeed, observations suggested that aggregation started within 1 hr whereas after the CNTs were sonicated in dilute acid, the suspensions remained stable over extended periods of time, up to several weeks. Even after only 10 min sonication, a large proportion of the CNT sample was dispersed although some agglomerates were noticed. The stability in chitosan solution both in suspension and during drying can also be seen.

As noted above, there have been a number of previous studies of sonochemical treatment of CNTs although those using acid etching of the surface have generally used much higher, more environmentally challenging conditions involving much higher concentrations. The untangling and deagglomeration resulting from microjets and fluid motion proceeds at a different rate than the oxidation and surface reorganisation. Physical damage such as shortening of the CNTs also occurs. Each of these may be needed to different extents depending on the final application and, as demonstrated here, both the treatment time and the ultrasound intensity used determine the extent of modification of the CNTs and hence have to be optimised for each particular case.

The 20 kHz horn used for sonication here would have produced relatively large cavitation bubbles and so maximized the physical effects such as shock waves and acoustic streaming. Cavitation produced using higher frequency ultrasound tends to produce less turbulence but greater production of radicals. Cravotto and co-workers [26] showed that sonication at 300 kHz in concentrated acids caused oxidation with less damage to the CNTs. It would be interesting to use higher frequency ultrasound under the milder conditions employed in this work. Alternatives could involve a short burst of 20 kHz ultrasound to disentangle the tubes and provide initial dispersion followed by longer sonication at high frequency to optimize the surface oxidation reactions.

3.2 Structural and mechanical analysis of Chi/CNT nanocomposites
Films of the chitosan composites were prepared by casting solutions and allowing them to dry in a dust-free atmosphere at room temperature. Films prepared from chitosan alone have poor mechanical integrity [27] and break during use so they usually have to be modified by adding fillers [18] or polymers [28]. Addition of the untreated CNTs used here was not found to be

useful as they formed large agglomerates and could not be dispersed evenly through the chitosan solution. Homogeneous dispersions could though be obtained using the sonochemically treated CNTs (Fig. 5 (c) and (d)).

The infra-red spectra of films cast from chitosan (Chi) and nanocomposites of chitosan containing treated CNTs (Chi/CNTs; CNTs reacted for 30 min at 12 W cm^{-2}) are shown in Fig. 6(a). For chitosan, characteristic peaks can be seen around 1649 (amide-I), 1571 (amide-II) and 1378 (amide-III) cm^{-1} [29]. In the spectrum of nanocomposites these peaks are shifted suggesting interaction of these groups which provides the stability of the dispersion. The characteristic peak of CNTs can also be seen around 2162 cm^{-1}. The effect of the CNT filler can clearly be seen in Fig. 6(b) which shows the stress-strain curves for unfilled chitosan and for films containing CNTs that had been sonochemically treated for 30 min at the three indicated intensities. The unfilled chitosan had a very low modulus and broke at low stress. Conversely, filled films were much stronger and could withstand deformation without breaking. The values of tensile strength and elongation at break derived from the data are shown in Table 2.
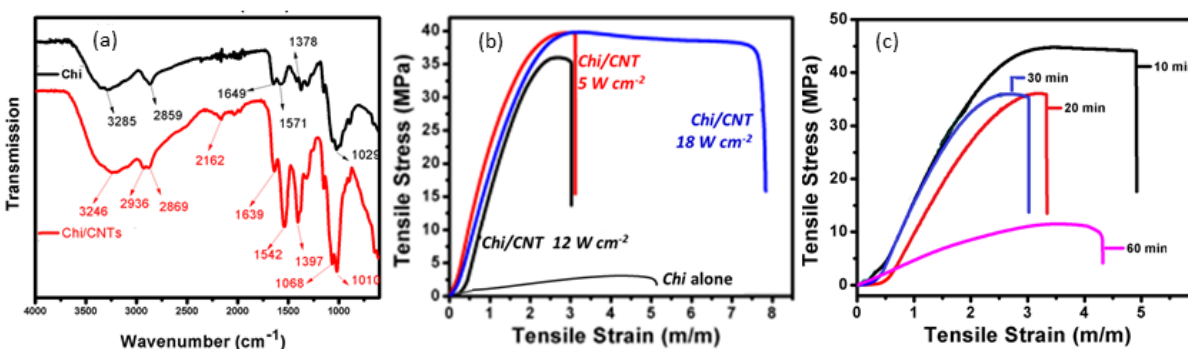

Figure 6: (a) Infra-red spectra of films of chitosan and chitosan-CNT nanocomposite (30 min at 12 W cm^{-2}); (b, c) stress-strain curves for chitosan and nanocomposites from sonochemically treated CNTs.

Table 2: Mechanical properties of CNT filled chitosan films

Sample Conditions	Tensile Strength / MPa	Elongation at break / %	Toughness / J m^{-3}
Chitosan	4.13	293	6.96
30 min at 5 W cm^{-2}	39.72	312	84.74
30 min at 12 W cm^{-2}	35.98	256	66.21
30 min at 18 W cm^{-2}	39.82	783	259.5
10 min at 12 W cm^{-2}	44.73	492	157.6
30 min at 12 W cm^{-2}	35.92	334	65.62
60 min at 12 W cm^{-2}	11.51	432	33.62

The results show considerable variation with both treatment time and the intensity of ultrasound used. While further data would be required to confirm the hypothesis, there appears to be an optimum intensity. It seems reasonable to assume that increasing the ultrasound intensity would initially increase the effect due to greater numbers of cavitation bubbles and higher shear/microjetting. However, above a certain value some of the effect is lost, presumably due to the extensive damage and agglomeration caused at the highest intensity observed above (Fig. 1, 18 W cm^{-2}). Similar comments can be made concerning the variation with time for samples sonicated at 12 W cm^{-2}. Although there is some variation in the results, the highest values of stress before breakage are obtained for those samples sonicated for short periods of time. This implies some interaction between filler and chitosan matrix but the interaction is not too strong to prevent some flexibility within the composite structure. The beneficial effect is gradually lost with further treatment (although still vastly exceeding those for unfilled chitosan). The increased mechanical strength is due in large part to the excellent solubility and dispersion of CNTs into

the chitosan matrix aided by the presence of oxygen functionalities which also facilitate favourable interaction between the filler and the matrix.

3.3 Preparation and application of functional membranes

The ultimate aim of modifying the CNTs is to enable their use as functional fillers in multicomponent films. Two examples from work using these films as supports for sonochemically generated nanoparticles will serve to illustrate their applications as catalytic systems.

Nanocomposite films were prepared containing iron oxide in the form of magnetite. In addition to the potential reactivity of the Fe_3O_4, this would make the film magnetic, significantly easing its recovery in catalytic or related applications. TEM indicated that the Fe_3O_4-NPs were in the region of $10 - 15$ nm in diameter (Fig. 7(a)). The Fe_3O_4-NPs and CNTs showed good dispersion in a chitosan matrix Fig. 7(a)) with good separation in both cases. Fig. 7(c) shows the dry films of Chi/ Fe_3O_4 and Chi/ Fe_3O_4/CNTs indicating that the fillers were well dispersed and that the film forming ability was not compromised by including Fe_3O_4-NPs.

Morphological characterization of the nanocomposite films was conducted using SEM, illustrated in Fig. 7(d, e) and showed the typical fractured surface of chitosan nanocomposites. The film is more continuous and less porous when the CNTs are included although even without the CNTs a well structured film could be formed. This shows the strong interactions between Fe_3O_4 –chitosan and also between the CNTs and chitosan as noted above. The tensile strength of the nanocomposites films was determined in order to investigate the effect of adding Fe_3O_4 and CNTs on the tensile properties of chitosan. Fig. 7(g) shows the tensile stress-strain curves for both films. For both samples the tensile stress increased linearly with strain in early stages but

17

the tensile strength of nanocomposite containing CNTs is much greater than that where no CNTs are included and the film extensible to a greater extent before breakage.

The catalytic activity of the nanocomposites films was evaluated using the reduction of methylene blue dye in the presence of $NaBH_4$ at room temperature. The progress of the reaction was monitored by UV-vis spectrophotometry as shown in Fig. 8. The peak at 663 nm corresponding to methylene blue gradually reduced in intensity and disappeared within 24 h to leave a colourless solution. No reaction was detected using Chi/CNT films with no iron oxide incorporated. It was observed that the reactivity of nanocomposite films both with and without CNTs were very similar, indicating that the Fe_3O_4-NPs were promoting the reaction of borohydride and that the methylene blue was not simply adsorbing onto the CNTs, However, the CNT containing films had much better mechanical integrity and were therefore more suitable for long term use. Although under these conditions the reaction is slow and would not find commercial use, it establishes the possibility in principle of using a magnetic, catalytically active film based on a chitosan matrix.

As a second example of the application of our nanocomposites, films containing gold dispersed on CNTs were prepared and employed as catalysts [17]. Nanoparticulate gold has been widely used as an efficient catalyst, particularly supported on a matrix so that the nanostructure can be retained [30]. Chitosan films containing our modified CNTs with sonochemically generated Au-NPs were tested for this purpose using a model reaction, the hydrogenation of 4-nitrophenol to give 4-aminophenol using sodium borohydride, a comparatively mild and clean reducing agent.
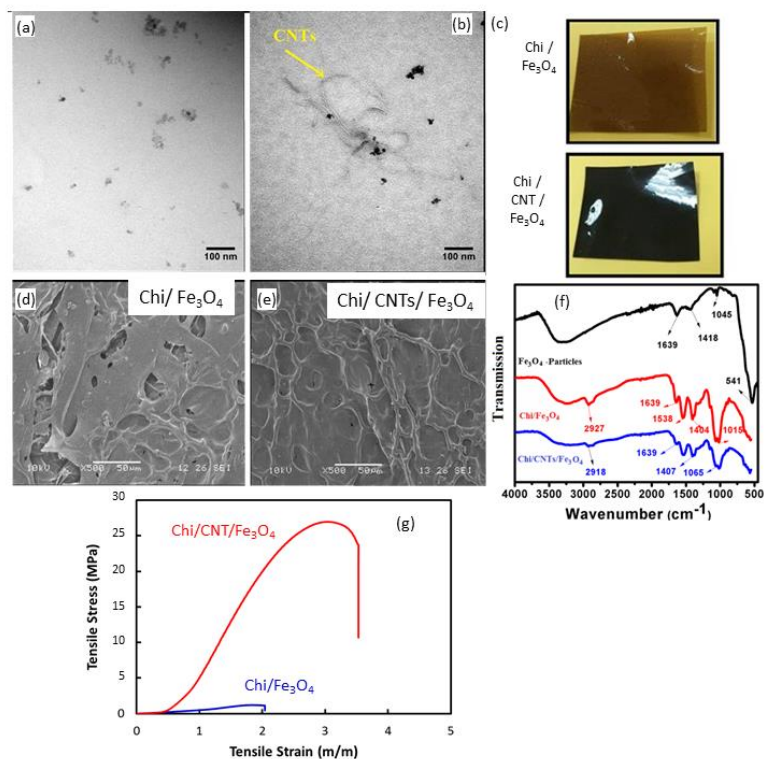
Figure 7: TEM images of (a) Fe$_3$O$_4$-NP and (b) Fe$_3$O$_4$-NPs/Chi//CNT nanocomposite; (c) photographs of nanocomposite films; (d), (e) SEM images of nanocomposite films; (f) FTIR spectra of Fe$_3$O$_4$-NP and Fe$_3$O$_4$-NPs/Chi//CNT nanocomposite; (g) stress strain curves for nanocomposite films
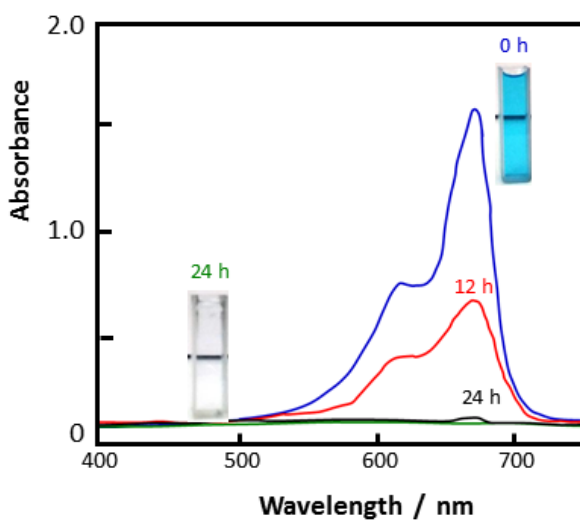

Figure 8: UV-visible spectra of methylene blue solutions after exposure to chitosan – CNT - Fe$_3$O$_4$-NP nanocomposites

As with the Chi/ Fe_3O_4/CNTs systems, electron microscopy indicated that both nanocomposites were porous although the pore size was larger in Chi/Au than Chi/Au/CNTs. Chi/Au/CNTs had a more compact structure which also resulted in increased mechanical strength of the nanocomposite films. FTIR spectra again suggested that the complexation of Au-NPs occurred through the amine and amide groups of the chitosan [17].

The films were active as catalysts as shown in Fig. 9(a). The mixture of 4-NP and $NaBH_4$ showed a λ_{max} at 400 nm. In the absence of gold, the solution was stable and unreactive over a period of several hours. On adding a small piece of nanocomposite membrane, the absorbance fell over around five minutes with a corresponding increase in the absorbance at ∼ 320 nm attributable to the product amino phenol. Using the Chi/Au/CNTs film accelerated the reaction and reduction was complete in under three minutes, mainly due to reducing the induction period before the reduction commenced (Fig. 9(b)). The main difference was that the inclusion of CNTs significantly improved the mechanical properties of the film so that it would be reused with no loss of gold for over 10 repeat cycles whereas films with no CNTs lost their integrity after being used twice (Fig. 9 (c)).
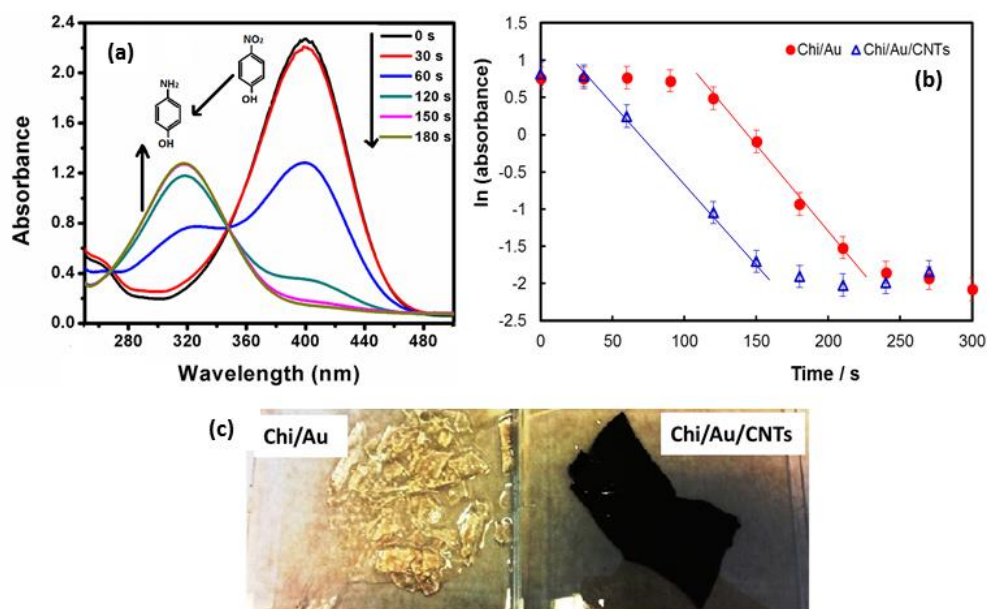
Figure 9: Borohydride reduction of 4-nitrophenol at room temperature catalysed by supported Au-NPs [17]. (a) UV-Vis Spectra using Chi/Au/CNTs (b). First order rate plots (c). Photographs of nanocomposite membranes Chi/Au after two reaction cycles and Chi/Au/CNTs after 10 cycles.

Conclusions

A systematic study of the effect of ultrasound assisted acid oxidation on MW-CNTs and the implications of their use as functional fillers in chitosan films has been conducted. Significant modification of the structure of the CNTs and their surface chemistry was found while using much lower acid concentrations than are usually reported. Changes in the structure and morphology of the CNTs have been measured. Treatment in dilute acid initially leads to a slight reduction in the level of disorder and defects in the structure as revealed by Raman spectroscopy

although these factors can be increased at extended treatment times. The introduction of oxygenated species at the surface was detected by FTIR spectroscopy. The observed effects could be correlated with the time and intensity of the ultrasound used and clearly showed that optimum conditions occur beyond which the benefit of using ultrasound reduces. Our results illustrate the importance of careful control over these parameters if optimum results are to be obtained. The CNT modifications lead to enhanced mechanical properties such as strength and extensibility when incorporated into chitosan films making them more robust and enhancing their usefulness. Our work also demonstrates that sonochemically generated nanoparticles can be incorporated into the films to add functionality.

References

1. P.J.F Harris *Carbon Nanotube Science: Synthesis, Properties and Applications* Cambridge University Press (2009) ISBN: 9780521828956

2. D.R. Barbero, S.D. Stranks, Functional Single-Walled *Carbon Nanotubes and Nanoengineered Networks for Organic‐and Perovskite‐Solar‐Cell Applications*, Adv. Mater. 28 (2016) 9668-9685

3. N. Selvakumar, A. Biswas, D.S. Rao, S. Krupanidhi, H.C. Barshilia, *Role of component layers in designing carbon nanotubes-based tandem absorber on metal substrates for solar thermal applications*, Solar Energy Materials and Solar Cells, 155 (2016) 397-404.

4. M. Arjmand, K. Chizari, B. Krause, P. Pötschke, U. Sundararaj, *Effect of synthesis catalyst on structure of nitrogen-doped carbon nanotubes and electrical conductivity and electromagnetic interference shielding of their polymeric nanocomposites,* Carbon, 98 (2016) 358-372.

5. B. Galindo, A. Benedito, E. Gimenez, V. Compañ, *Comparative study between the microwave heating efficiency of carbon nanotubes versus multilayer graphene in polypropylene nanocomposites*, Composites Part B: Engineering, 98 (2016) 330-338.

6. X. Wu, C. Lu, Y. Han, Z. Zhou, G. Yuan, X. Zhang, *Cellulose nanowhisker modulated 3D hierarchical conductive structure of carbon black/natural rubber nanocomposites for liquid and strain sensing application,* Composites Science and Technology, 124 (2016) 44-51.

7. Y. Wang, J. Wu and F. Wei, *A treatment method to give separated multi-walled carbon nanotubes with high purity, high crystallization and a large aspect ratio* Carbon, 41 (2003) 2939-2948.

8. H. Hiura, T. Ebbesen, J. Fujita, K. Tanigaki and T. Takada, *Role of sp3 defect structures in graphite and carbon nanotubes* Nature, 367 (1994) 148-151.

9. Y. Yan,J. Miao,Z. Yang,F.X. Xiao,H.B. Yang,B. Liu and Y. Yang *Carbon nanotube catalysts: recent advances in synthesis, characterization and applications* Chem. Soc. Rev., (2015) 44 3295-3346

10. S. Bibi, T. Yasin, S. Hassan, M. Riaz, M. Nawaz, *Chitosan/CNTs green nanocomposite membrane: Synthesis, swelling and polyaromatic hydrocarbons removal*, Materials Science and Engineering: C, 46 (2015) 359-365.

11. R. Tian, S. Liang, G. Li, Y. Zhang, L. Shi *Comparatively studying the ultrasound present in a mild two-stage approach on the content of functional groups in modified MWCNT* Chem. Phys. Lett. 650 (2016) 11–15

12. C.M. Ng, S. Manickam *Improved functionalization and recovery of carboxylated carbon nanotubes using the acoustic cavitation approach* Chem. Phys. Lett. 557 (2013) 97–101

13. K. S. Suslick and G. J. Price, *Applications of Ultrasound to Materials Chemistry* Annual Review of Materials Science, 29 (1999) 295-326.

14. S. Manickam, M. Ashokkumar (Eds) *Cavitation: A novel Energy-efficient teachnique for the generation of nanomaterials* Pan Stanford Singapore 2014.

15. R. Gusmão, M. Melle-Franco, D. Geraldo, F. Bento, M.C. Paiva, F. Proença, *Probing the surface of oxidized carbon nanotubes by selective interaction with target molecules*, Electrochemistry Communications, 57 (2015) 22-26.

16. S. Bibi, M. Nawaz, T. Yasin, M. Riaz, *Chitosan/CNTs nanocomposite as green carrier material for pesticides controlled release,* Journal of Polymer Research, 23 (2016) 154.

17. S.Bibi, G.J. Price, T. Yasin, M. Nawaz *Eco-friendly synthesis and catalytic application of Chitosan/Gold/ Carbon Nanotube nanocomposite films* RSC Advances 6, 60180 – 60186 (2016)

18. H. Tamura, T. Furuike, *Chitin and Chitosan*, Encyclopedia of Polymeric Nanomaterials, (2015) 386-389.

19. M. Oh, F. Sun, H.-R. Cha, J. Park, J. Lee, M. Kim, K.-B. Kim, S.H. Kim, J. Lee, D. Lee, *Vertically aligned multi-layered structures to enhance mechanical properties of chitosan– carbon nanotube films*, J. Mater. Sci., 50 (2015) 2587-2593.

20. X-P. Wei, Y.-L. Luo, F. Xu, Y.-S. Chen, L.-H. Yang, *In-situ non-covalent dressing of multi-walled carbon nanotubes@ titanium dioxides with carboxymethyl chitosan nanocomposite electrochemical sensors for detection of pesticide residues*, Mater. Des., 111 (2016) 445-452.

21. S. Koda, T. Kimura, T. Kondo, H. Mitome, *A standard method to calibrate sonochemical efficiency of an individual reaction system* Ultrason. Sonochem., 10 (2003) 149-156

22. W. Huang, Y. Lin, S. Taylor, J. Gaillard, A. M. Rao and Y.-P. Sun, *Sonication-Assisted Functionalization and Solubilization of Carbon Nanotubes* Nano Letters, **2** (2002) 231-234

23. C. Yang, X. Hu, D. Wang, C. Dai, L. Zhang, H. Jin and S. Agathopoulos, *Ultrasonically treated multi-walled carbon nanotubes (MWCNTs) as PtRu catalyst supports for methanol electrooxidation* J.Power Sources, **160** (2006) 187-193.

24. A. Jorio, M.S. Dresselhaus, R. Saito, G. Dresselhaus *Raman Spectroscopy in Graphene Related Systems* Wiley-VCH: Weinheim, Germany, 2011.

25. F.A. Sheikh, J. Macossay, T. Cantu, X. Zhang, M.S. Hassan, M.E. Salinas, C.S. Farhangi, H. Ahmad, H. Kim, G.L. Bowlin, *Imaging, spectroscopy, mechanical, alignment and biocompatibility studies of electrospun medical grade polyurethane (Carbothane™ 3575A) nanofibers and composite nanofibers containing multiwalled carbon nanotubes*, Journal of the mechanical behavior of biomedical materials, 41 (2015) 189-198.

26. G. Cravotto, D.de Garella, E.C. Gaudino, F. Turci, S. Bertarione,G. Agostini, F. Cesano and D. Scarano *Rapid purification/oxidation of multi-walled carbon nanotubes under 300 kHz-ultrasound and microwave irradiation* New J. Chem. 35 (2011) **915-919**

27. C. Caner, P. J. Vergano, and J. L. Wiles *Chitosan Film Mechanical and Permeation Properties as Affected by Acid, Plasticizer, and Storage* J. Food Sci. 63(6) (1998) 1049 - 1053

28. V.L. Alexeev, E.A. Kelberg, G. A. Evmenenko, S.V. Bronnikov, *Improvement of the mechanical properties of chitosan films by the addition of poly(ethylene oxide)*. Polym Eng Sci, 40 (2000) 1211–1215

28. I. Aranaz, M. Mengibar, R. Harris, I. Panos, B. Miralles, N. Acosta, G. Galed and A. Heras, *Functional characterization of chitin and chitosan*, Current Chemical Biology, 3 (2009) 203-230

30. G. J. Hutchings, *Catalysis by gold* Catalysis Today **100** (2005) 55–61.